Nuclear Instruments and Methods in Physics Research A 796 (2015) 118–125

Contents lists available at ScienceDirect

Nuclear Instruments and Methods in Physics Research A

journal homepage: www.elsevier.com/locate/nima

Charge collection in Si detectors irradiated *in situ* at superfluid helium temperature

Elena Verbitskaya [a,*], Vladimir Eremin [a], Andrei Zabrodskii [a], Bernd Dehning [b], Christoph Kurfürst [b], Mariusz Sapinski [b], Marcin R. Bartosik [b], Nicolai Egorov [c], Jaakko Härkönen [d]

[a] Ioffe Institute, 26 Politekhnicheskaya str., St. Petersburg 194021, Russian Federation
[b] CERN, CH-1211, Geneva 23, Switzerland
[c] Research Institute of Material Science and Technology, 4 Passage 4806, Moscow, Zelenograd 124460, Russian Federation
[d] Helsinki Institute of Physics, P.O.Box 64 (Gustaf Hallströmin katu 2) FI-00014 University of Helsinki, Finland

ARTICLE INFO

Available online 20 March 2015

Keywords:
Large hadron collider
Beam loss monitoring
Radiation hardness
Charge collection
Superfluid helium

ABSTRACT

Silicon and diamond detectors operated in a superfluid helium bath are currently being considered for the upgrade of the LHC beam loss monitoring system. The detectors would be installed in immediate proximity of the superconducting coils of the triplet magnets. We present here the results of the *in situ* irradiation test for silicon detectors using 23 GeV protons while keeping the detectors at a temperature of 1.9 K. Red laser (630 nm) Transient Current Technique and DC current measurements were used to study the pulse response and collected charge for silicon detectors irradiated to a maximum radiation fluence of 1×10^{16} p/cm^2. The dependence between collected charge and irradiation fluence was parameterized using the Hecht equation and assumption of a uniform electric field distribution. The collected charge was found to degrade with particle fluence for both bias polarities. We observed that the main factor responsible for this degradation was related to trapping of holes on the donor-type radiation-induced defects. In contrast to expectations, along with formation of donors, acceptor-type defects (electron traps) are introduced into the silicon bulk. This suggests that the current models describing charge collection in irradiated silicon detectors require an extension for taking into account trapping at low temperatures with a contribution of shallow levels. New *in situ* irradiation tests are needed and planned now to extend statistics of the results and gain a deeper insight into the physics of low temperature detector operation in harsh radiation environment.

1. Introduction

The High-Luminosity upgrade of the LHC (HL-LHC) aims at a tenfold increase of beam luminosity [1]. In this case both the collider machine and the experimental facilities will undergo major upgrades. The higher luminosity emphasizes the importance of a reliable Beam Loss Monitoring System whose main purpose is machine protection from the beam losses and especially quench prevention of the superconducting magnet coils. The present configuration of the LHC beam loss monitors (BLMs) based on ionization chambers placed outside the magnet cryostat makes it difficult to estimate exactly energy deposition in the coils due to the debris which masks the beam loss signal [2]. The alternative option suggested by the CERN-BE-BI-BL group [3,4] for the HL-LHC is based on the application of semiconductor detectors located as close as possible to the superconducting coils of the magnets. These detectors, preferably silicon and diamond ones, will be immersed in superfluid helium and operate at a temperature T of 1.9 K. Silicon detectors have the advantage of well-developed technology for mass-production, low production costs and a well-known behavior when irradiated. One point that has still to be addressed is whether silicon detectors can withstand high radiation environment when being immersed in superfluid helium. The models of radiation damage predict a different defect behavior at LHe temperature when compared to room temperature (*RT*). Among the primary defects in silicon, only interstitials are mobile at $T\sim4$ K and can participate in the creation of interstitial-related defect complexes (mainly donor-type defects), whereas primary vacancies are immobile at such low T [5,6]. This hinders from the introduction of vacancy-related acceptor-type defects (VV, V_2O, *etc.*), which control the accumulation of negative charge in the detector bulk and are responsible for the degradation of silicon detector characteristics, including charge collection. This gives us hope that the radiation hardness of silicon detectors will be adequate in superfluid helium media. The study of this issue was the aim of the *in situ* irradiation test.

* Corresponding author. Tel.: +7 812 292 7953; fax: +7 812 249 1017.
E-mail address: elena.verbitskaya@cern.ch (E. Verbitskaya).

http://dx.doi.org/10.1016/j.nima.2015.03.027
0168-9002/

The work on this project started at CERN in 2011 included tests of nonirradiated silicon and diamond detectors operating at ~2 K and *in situ* irradiation test of these detectors at 1.9 K [7–9]. Irradiation test was performed at the CERN PS beam line where the detectors were irradiated with 23 GeV protons. A detailed description of the *in situ* experiment and the characterization of irradiated detectors are given in [9]. The collected charge Q_c was derived from the data on the detector DC current induced by proton spills, and the dependences of the charge on the bias voltage V and irradiation fluence F were obtained and qualitatively explained.

In this work the results of the *in situ* irradiation test of silicon detectors operated at 1.9 K undergo extended analysis. The data on the current pulse response changes with accumulated fluence are described. An approximation of $Q_c(F)$ dependences is performed using the Hecht equation. The aim is the estimation of the trapping effects and possible electric field transformations under irradiation at 1.9 K. We analyze the experimental results looking for specific features of radiation-induced defect formation at such low temperature.

2. Experimental conditions

The investigated silicon detectors were p^+–n–n^+ structures processed on wafers with a resistivity of 10 kΩ cm, 500 Ω cm and 4.5 Ω cm and a thickness of 300 μm. The sensitive area was 5×5 mm^2 for the samples used in the measurements of collected charge and 1×1 mm^2 in a single sample for which the current pulse response was measured [9].

Irradiation of the detectors was carried up to the maximum fluence of 1×10^{16} p/cm^2. The measurement points were within the range 5×10^{13}–1×10^{16} p/cm^2, being different for taking TCT and DC current data. The error in the fluence estimation was ±7% [10].

The current pulse response was measured using the Transient Current Technique (TCT) [11] with a LeCroy WavePro 7300A oscilloscope with a 3 GHz analog bandwidth and a sampling rate of 10 GS/s. A red laser with a 630 nm wavelength was applied to induce the transient charge in the detector. The laser pulse width was 45 ps and the diameter of the light spot was 1 mm. The laser frequency was 10 kHz, and in some cases 100 Hz, in order to estimate a possible influence of the charge generated by the laser on the pulse signal. Because of the technical problems with the radiation hardness of the cables used in the TCT measurements [9], the pulse signal was recorded only from the back n^+ side. To assure a proper spread resistance of the surface at 1.9 K, the aluminum contact in this detector was made as a mesh.

Special attention was paid to the reduction of pickup in the pulse signals. Since the measurement apparatus for TCT was located at a distance of 12 m from the cryostat in which the detectors were installed, the pickup and noise disturbed a small signal of irradiated detector. This restricted the sensitivity of the TCT measurements for detectors irradiated beyond $(5–7) \times 10^{14}$ p/cm^2.

The collected charge was determined by an integrating the detector output DC current induced by the proton beam and measured by a current meter [9]. Integration was made over 20 proton spills, the duration of each being 400 ms. To avoid a systematic error, the current was measured and averaged within a random 16.67 ms period and an interval of 60 ms between the records. In this case a statistical error of the estimated charge was ±15%. The measurements were performed for detectors irradiated up to 1×10^{16} p/cm^2.

The data were recorded at both reverse and forward bias, V_{rev} and V_{forw}, respectively, in the interval 50–500 V, the latter mode corresponding to the detector operation as a current injected detector (CID) [12].

It should be noted that this was the first *in situ* radiation test at 1.9 K, therefore it was difficult to anticipate all issues in the experiment, which explains why not all measurements and obtained results are systematic.

3. Evolution of the current pulse response under *in situ* irradiation at 1.9 K

3.1. Electric field distribution in silicon detectors irradiated at 1.9 K

The detector operation is controlled by two factors: the electric field distribution $E(x)$ in the detector bulk (x is the coordinate), and transport properties of the radiation generated nonequilibrium carriers, *i.e.* their mobility and trapping parameters. The main source of information on the electric field distribution is the study of the current pulse response using TCT [11]. In the case of a nonirradiated silicon detector with the trapping time constant τ significantly exceeding the charge collection time t_{col}, it is possible for the $E(x)$ profile to be reconstructed from the detector current pulse response initiated by generation of the electron–hole (e–h) pairs in a narrow layer adjacent to one of the detector contacts. The same can be achieved for a detector irradiated below $(5–7) \times 10^{14}$ p/cm^2 [13,14]. For detectors processed from high-resistivity detector grade silicon the experimental data, including the measurements at 1.9 K, show well predictable shapes of the pulse responses which correspond to a nearly constant electric field and a negligible density of space charge [8]. This result indicates that at $T=1.9$ K the carriers at the energy levels in the detector bulk are frozen. This also applies to shallow levels of donors (phosphorus) and acceptors (boron), whose activation energies are 45 meV. Obviously, in pure and nonirradiated Si the concentration of the centers responsible for the bulk generated current is extremely low, and trapping of the carriers from this current does not affect the electric field distribution differently from what is observed in irradiated Si detectors operated at *RT* [13].

Before the presentation and discussion of the TCT data, it is important to determine the steady-state electric field distribution at 1.9 K in irradiated detectors without externally induced free carrier generation. Although a low bulk current is indication of a small concentration of deep energy levels (DLs), we cannot infer from this the free carrier trapping effect to be small as well. Indeed, the detrapping probability $1/\tau$ from the trapping centers with DLs is also close to zero at 1.9 K, therefore the balance of emission and capture processes can be hardly predicted. To estimate the $E(x)$ distribution in irradiated silicon detectors, we extended simulation of the $E(x)$ profile developed for detectors operated at *RT* [13] to the LHe conditions, keeping the same spectra of the effective DLs and changing the operational temperature. *E.g.*, the calculated $E(x)$ profiles in the detector operated at V_{rev} of 300 V and irradiated to 5×10^{15} p/cm^2 are depicted in Fig. 1 at T of 200–4 K. The profile has a double peak (DP) shape at $T=200$ K. At $T=100$ K and below the electric field

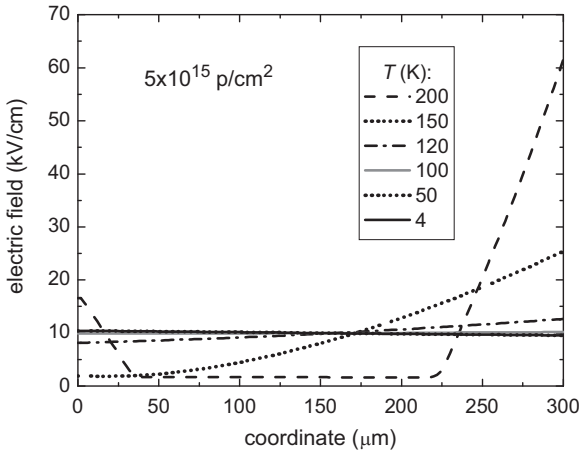

Fig. 1. Calculated electric field distributions in the detector irradiated at 1.9 K. $V_{rev}=300$ V, $F=5 \times 10^{15}$ p/cm^2; $x=0$ is at the p^+ contact.

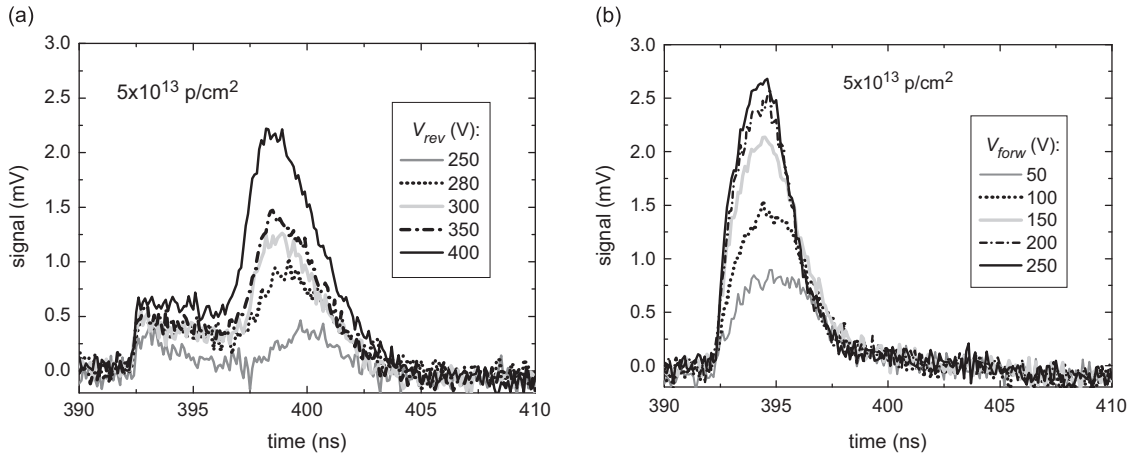

Fig. 2. Current pulse response of the detector irradiated to 5×10^{13} p/cm^2 at 1.9 K and operated at reverse (a) and forward (b) bias voltages.

becomes practically uniform and equals $V/d \approx 1 \times 10^4$ V/cm, *i.e.* space charge is close to zero due to full compensation of charged DDs and DAs and freezing of trapped carriers. The calculations made at $T \leq 100$ K show the same uniform profile in the detectors irradiated in the fluence range 5×10^{13}–1×10^{16} p/cm^2. At the same time, the simulated current pulses due to hole drift (laser illuminates the n^+ side, V_{rev}) in the detectors irradiated to fluences below 1×10^{14} p/cm^2 have a flat top. The decay in the transient current shape is observed at $F \geq 5 \times 10^{14}$ p/cm^2, which is caused by the degradation of the trapping time constant.

3.2. Current pulse response of silicon detectors irradiated at 1.9 K

The pulse signals described in this section were measured in the intervals between spills. The current pulse responses of the detector irradiated to 5×10^{13} p/cm^2 and operated at reverse and forward bias are shown in Fig. 2. For a better visualization, the signals are shown in the same polarity (*i.e.* at V_{forw} the transient current is actually negative). The response is measured from the n^+ side, and at V_{rev} it corresponds to the drift of nonequilibrium holes generated by a light pulse from the n^+ contact to the p^+ contact (Fig. 2a), and at V_{forw} to the drift of electrons in the same direction (Fig. 2b). In the first case the pulse has a DP shape with the increasing right peak, which is the evidence for a nonuniform $E(x)$ distribution with two maxima at the p^+ and n^+ contacts, a lower field being near the n^+ contact. This response shape is typical of irradiation at *RT* to the medium fluence before the space charge sign inversion (SCSI) and the following measurements at *RT* or at slight cooling. Systematic evolution of the response shapes is observed in a wide range of bias.

These experimental results contradict the calculated $E(x)$ profiles at LHe temperature (Fig. 1) and the corresponding pulse shapes, which can be ascribed to the experimental conditions. The detector was irradiated under reverse bias of 100 V (which corresponds to its operation as BLM), and then the TCT measurements were performed during a period of several minutes preceding the arrival of the following spill. Thus, electrons and holes which contribute to the detector reverse current generated during the spill will be trapped on the defects levels nonuniformly over the detector bulk, with dominating concentration of trapped electrons near the n^+ contact and holes near the p^+ contact [15]. Such trapping leads to formation of regions with a stronger electric field at both contacts, which qualitatively corresponds to the observed current pulse response shapes.

Inverting the bias polarity changes significantly the pulse shapes (Fig. 2b). The front of the pulse shows an extended rise, which indicates a low electric field at the n^+ contact with its progressive growth towards the opposite p^+ contact. This feature correlates to the electric field distribution in CIDs which operate at forward bias [12]. In this mode the electric field at the contact which gives injection of the current (in our case the n^+ contact injects electrons) falls to zero, and the current is limited by the space charge trapped in the bulk (Space Charge Limited Current (SCLC) mode) [16]. The electric field is rising inside the bulk towards the p^+ contact as $\sqrt{x}$ (in this case $x=0$ at the n^+ contact) at any bias. However, at low voltages the specific shape is not very pronounced due to trapping of the collected electrons, which cut out the peak at the descending edge of the response, and the current pulse responses do not have the DP shape.

At F of 2.7×10^{14} p/cm^2 the current pulse responses at V_{rev} (Fig. 3a) have shapes different from those in Fig. 2a. A sharp rise to the maximum amplitude and the following decay indicate that the electric field maximum E_{max} is near the n^+ contact, *i.e.* SCSI occurred in the fluence interval between the previous and this measurement. This implies that formation of acceptor-type vacancy-related defects under irradiation takes place with an introduction rate comparable with or higher than the rate of donor-type defects introduction. In detectors processed from 10 kΩ cm FZ n-type silicon the estimated fluence at which SCSI occurs at *RT*, F_{inv}, is about $(1–3) \times 10^{13}$ p/cm^2. Hence, at 1.9 K this inversion is likely to be delayed. The second peak is not observed anymore, which is the evidence for the reduction of the trapping time constant of holes τ_h leading to the relationship $\tau_{tr} < t_{col}$.

The pulse shapes at forward bias (Fig. 3b) differ from those at V_{rev}. At V_{forw}=400–500 V the responses have an almost flat top followed by a sharp decay. Such difference indicates that electrons drift throughout the entire detector and reach the p^+ contact, *i.e.* the electron trapping time constant τ_e is greater than τ_h. However, the collected charge decreases at both polarities of the bias voltage, which is made evident by comparing the pulse amplitudes in Figs. 2 and 3.

After irradiation to 3.1×10^{14} p/cm^2 the pulse responses have descending shapes at both V_{rev} and V_{forw} (Fig. 3c and d, respectively). Though the difference in the fluence does not exceed 10%, the reduction of the pulse amplitudes is about 60% at both polarities of the bias, which may well be due to the reduction of the trapping time constants of electrons and holes. The decay of the pulse amplitude is sharper at V_{rev}, therefore the relationship $\tau_h < \tau_e$ holds. The rise time of the pulse responses from the detector operated at V_{forw} becomes shorter than from this detector irradiated to 2.7×10^{14} p/cm^2.

At $F \sim (5–7) \times 10^{14}$ p/cm^2 the detector signals drop significantly. The evolution of the current pulse response under irradiation is summarized in Fig. 4.

3.3. Influence of spill charge and laser frequency on the current pulse response

According to the measurements of the current pulse response of the detector irradiated *in situ*, two factors affect the shape and the value of the pulse signal. One is the charge generated in the detector

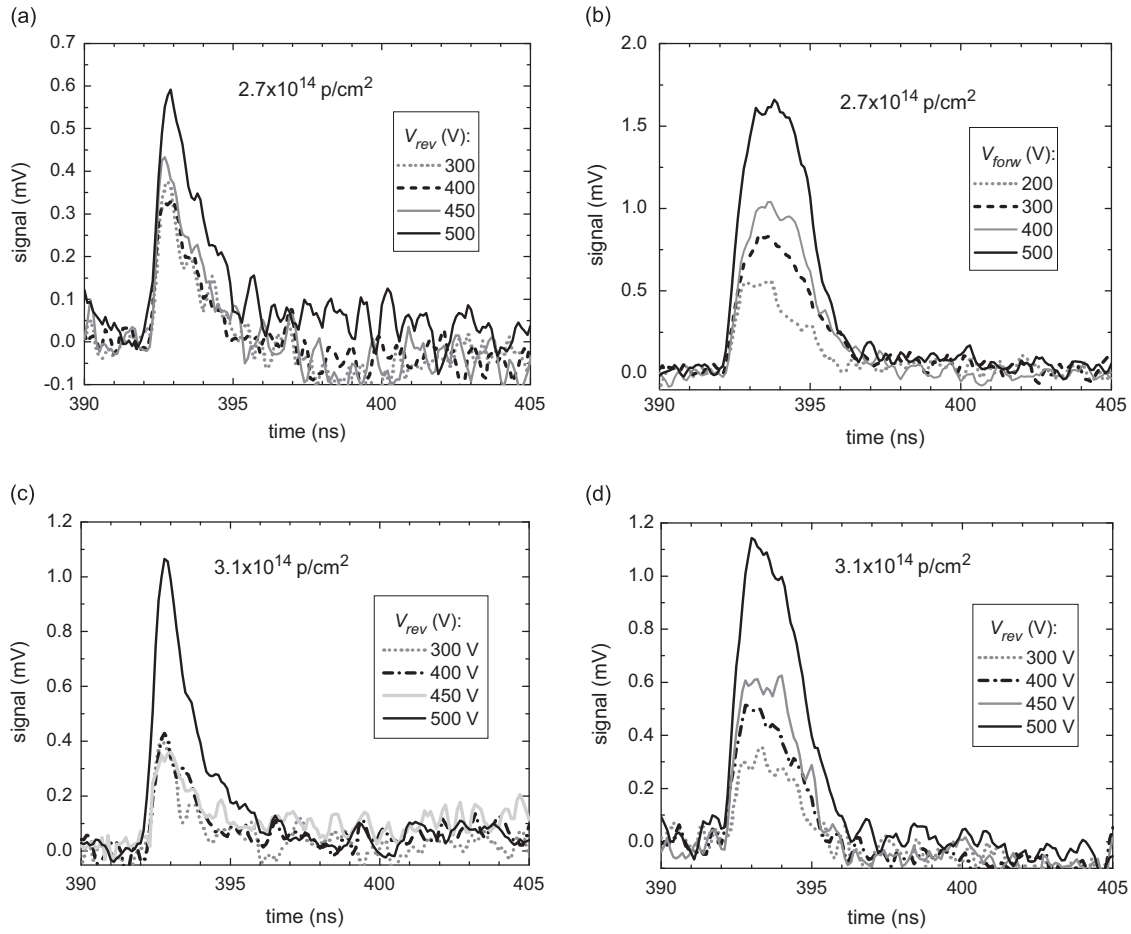

Fig. 3. Current pulse response of the detector irradiated to 2.7×10^{14} p/cm^2 at 1.9 K and operated at reverse (a and c) and forward (b and d) bias voltages.

by the spill. During the test the intensity of the proton beam was 1.3×10^{11} proton/cm^2 per 400 ms spill, corresponding to about 1×10^{10} proton/s on the detectors. For the detector under study this is equivalent to 1.3×10^{9} protons per 400 ms spill, *i.e.* the density of the current generated in the detector with a thickness of 300 μm is $\sim1\times10^{-3}$ A/cm^2. The study of the spill influence is of importance in practice as in the BLM operation this charge can affect the measured DC current which is actually the characteristic for estimating charge loss of the proton beam in LHC.

With the arrival of a spill the shapes and the amplitudes of the pulse responses immediately undergo significant changes. At the highest reverse bias of 450–500 V the pulse response of the detector irradiated to 2.7×10^{14} p/cm^2 reverts to a DP shape (Fig. 5a and c), which is different from the shapes shown in Fig. 3a. The appearance of the second peak in the pulse signal indicates an increase of τ_h and of the electric field at the p^+ contact. A specific feature of the pulse sequence in Fig. 5a is that the increase of the bias voltage leads to a systematic rise of the pulse amplitude, which is not the case with measurements made between the spills (Fig. 3a). The cause of this phenomenon is not quite clear yet. A possible explanation could be the changes in the properties of the energy levels of radiation-induced defects, such as their carrier capture cross-sections, which can change the occupancy of the defect levels and the charge density distribution inside the detector.

At V_{forw} the pulses acquire well defined shapes with a constant slope and a fast decay at $V_{forw}\geq400$ V (Fig. 5b and d). Similar shapes are typical of a nonirradiated silicon detector or a detector irradiated to a low *F*. In these cases the carrier trapping time constants are fairly large; an effective concentration in the space charge region, N_{eff}, is constant and controlled mainly by dopants, and the electric field distribution is linear. The changes of the pulse response at V_{forw} caused by spill charge show full depletion of the detector between 250 and 300 V and a threefold increase of the pulse amplitude; the latter indicates the rise of τ_e. At $V_{forw}=400$–550 V the pulse top is not flat anymore, as follows from the comparison with Fig. 3b. The top has a constant descending slope, indicating an increase of the negative N_{eff} in the detector sensitive bulk. Hence, at forward bias the carriers generated by the spill change the electric field near the n^+ contact, which becomes non-zero and extracts electrons from the contact inside the bulk. The electrons are captured on radiation-induced defects and, on the one hand, increase negative space charge. This leads to a linear electric field distribution in the SCR descending toward the p^+ contact. On the other hand, this capture reduces the concentration of traps, which results in the increase of the electron trapping time constant. Consequently, an enhancement of the pulse amplitude and collected charge takes place. It should be pointed out that charge introduced by spill does not affect the ratio between the trapping time constants ($\tau_h<\tau_e$). This follows from the comparison of Fig. 5c and d: even after the spill arrival the response shapes of the detector operated at V_{rev} have a gradual decay specific of a small τ.

The same changes of the pulse shape induced by spill charge are observed at higher irradiation fluences; the only specific feature is that at V_{forw} the negative slope of the response at the spill arrival increases with fluence. This is most likely to be due to a larger concentration of defects which capture electrons. However, the changes of the pulse response shapes stimulated by the spill arrival are not stable in time: the pulse amplitudes go down within a few seconds, and at V_{forw} the top of the pulse becomes flat, like it was before spill. Formally, it could be explained by emission of trapped

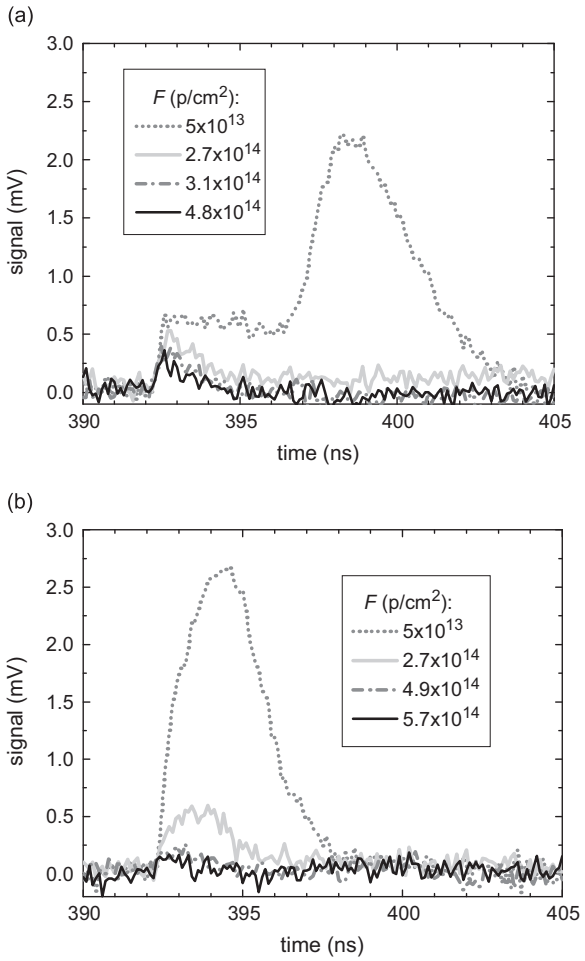

Fig. 4. Evolution of the current pulse response at reverse (a) and forward (b) bias voltage under *in situ* irradiation at 1.9 K. V_{rev}=400 V; V_{forw}=250 V.

electrons from the energy levels and reduction of the electric field near the n^+ contact. However, it is not clear why this emission occurs at such a low temperature.

The other factor affecting the pulse signal is the frequency f of the laser illuminating the detector. Systematic errors could be introduced by an excessive pulse frequency since the laser induces a quasi-DC carrier injection in the detector, whose current density j_{linj} is

$$j_{linj} = en_o f/S_o \quad (1)$$

where e is the elementary charge, n_o the number of electron–hole pairs generated by a single laser pulse and S_o the area of the light pulse spot. The current density equivalent to the laser generated current is 10^{-9} A/cm^2 at 100 Hz and 10^{-7} A/cm^2 at 10 kHz, which is significantly lower than that injected by spill. The carriers generated by a laser pulse are distributed within a thin layer near the n^+ contact, whose depth for a 630 nm wavelength is few μm (similar to the so-called "plasma state" in the track of ions due to electric field screening of electrons and holes [17]). Then the process of electron and hole separation and involvement in drift is similar to dispersal of the e–h plasma: the smaller is the e–h pair density, the greater is the amount of carriers flowing outside the near-surface layer and involved in the drift. This is the reason for a sharper rise of the signal at lower frequencies. As seen in Fig. 6a and b, the reduction of frequency from 10 kHz to 100 Hz in the absence of spill increases three-four times the amplitude of the signal of the detector irradiated to 4.9×10^{14} p/cm^2 at both bias polarities while holding its shape. A further reduction of frequency does not show any signal rise at $f\leq 50$ Hz.

The combined effect of two factors - spill generated charge in the total detector bulk and the changes in the concentrations of electrons and holes generated by laser near the n^+ contact with frequency reduction is also shown in Fig. 6a and b. In the measurements we first set the frequency and then measured the signal in the interval between spills and immediately after the arrival of a spill. Whereas at f= 10 kHz the spill generated charge gives a significant rise of signal, at f= 100 Hz the charge has practically no influence. These features are observed irrespective of the bias polarity. To explain the pulse shape changes due to a combined influence of spill charge and variation of frequency, one should take into account that the fluence of 4.9×10^{14} p/cm^2 is medium and the concentrations of radiation-induced defects cannot be high. Charged donors and acceptors will compensate each other leading to a uniform $E(x)$ distribution (Fig. 1). Before the spill arrival the pulse shape is governed by the trapping time constants which are already reduced as compared with their values before irradiation. This reduction is verified by the pulse response shapes with decay and the decrease of the pulse amplitudes. Nonequilibrium carriers introduced by spills are generated in the entire detector bulk, and both types of carriers drift towards the corresponding contacts and can be trapped. As seen in Fig. 5b, the N_{eff} becomes more negative. The carriers generated by light near the n^+ contact drift in the SCR and can also be trapped (trapped carriers are holes at V_{rev} and electrons at V_{forw}). A combined influence of nonequilibrium carrier trapping illustrated in Fig. 6, affects the response only at f= 10 kHz because the additional concentrations of electrons and holes at f= 100 Hz and further down are lower than those generated by the spill.

It should be noted that the increase of the signal stimulated by the spill arrival and measured at f= 10 kHz was observed in the detector under study in a limited fluence range. At $F=7.7\times10^{14}$ p/cm^2 the changes of the signal were insignificant at V_{forw}, whereas at V_{rev} the signal became negligible.

4. Simulation and fitting of $Q_c(F)$ dependences using the Hecht equation

Experimental dependences of the collected charge on the fluence and bias voltage in the reverse and forward bias modes, which were obtained in the test, were described in [9]. It was shown that at $F<1\times10^{15}$ p/cm^2 the rate of the collected charge degradation was higher at V_{forw} compared to that at V_{rev}, whereas the charge collected in detectors irradiated to the maximum fluence was insensitive to the bias polarity. The $Q_c(F)$ dependences for the detector processed from 10 kΩ cm silicon and operated at V_{rev} are depicted in Fig. 7. The curves here show that in the fluence range 1×10^{14}–1×10^{16} p/cm^2 the collected charge per minimum ionizing particle (MIP) is proportional to $F^{-0.5}$. For fitting were taken the $Q_c(F)$ dependences measured at the bias voltage of ±300 V.

The charge generated by MIPs and collected in the detector with a thickness d and a uniform electric field is described by the Hecht equation

$$Q_c = e\left[\frac{\mu_e V\tau_e}{d}\left(1-\frac{\mu_e V\tau_e}{w^2}\left(1-exp\left(-\frac{w^2}{\mu_e V\tau_e}\right)\right)\right)\right.$$
$$\left.+\frac{\mu_h V\tau_h}{d}\left(1-\frac{\mu_h V\tau_h}{w^2}\left(1-exp\left(-\frac{w^2}{\mu_h V\tau_h}\right)\right)\right)\right] \quad (2)$$

where V is the reverse bias voltage, w the depth of the space charge region (SCR), μ the carrier drift mobility, τ the trapping time constant, and the indexes e and h denote electrons and holes, respectively. This equation in our case gives the charge collected in a partially depleted detector with the SCR depth w in which for simplicity the electric field is also accepted to be uniform. The trapping time constants are the parameters with the following

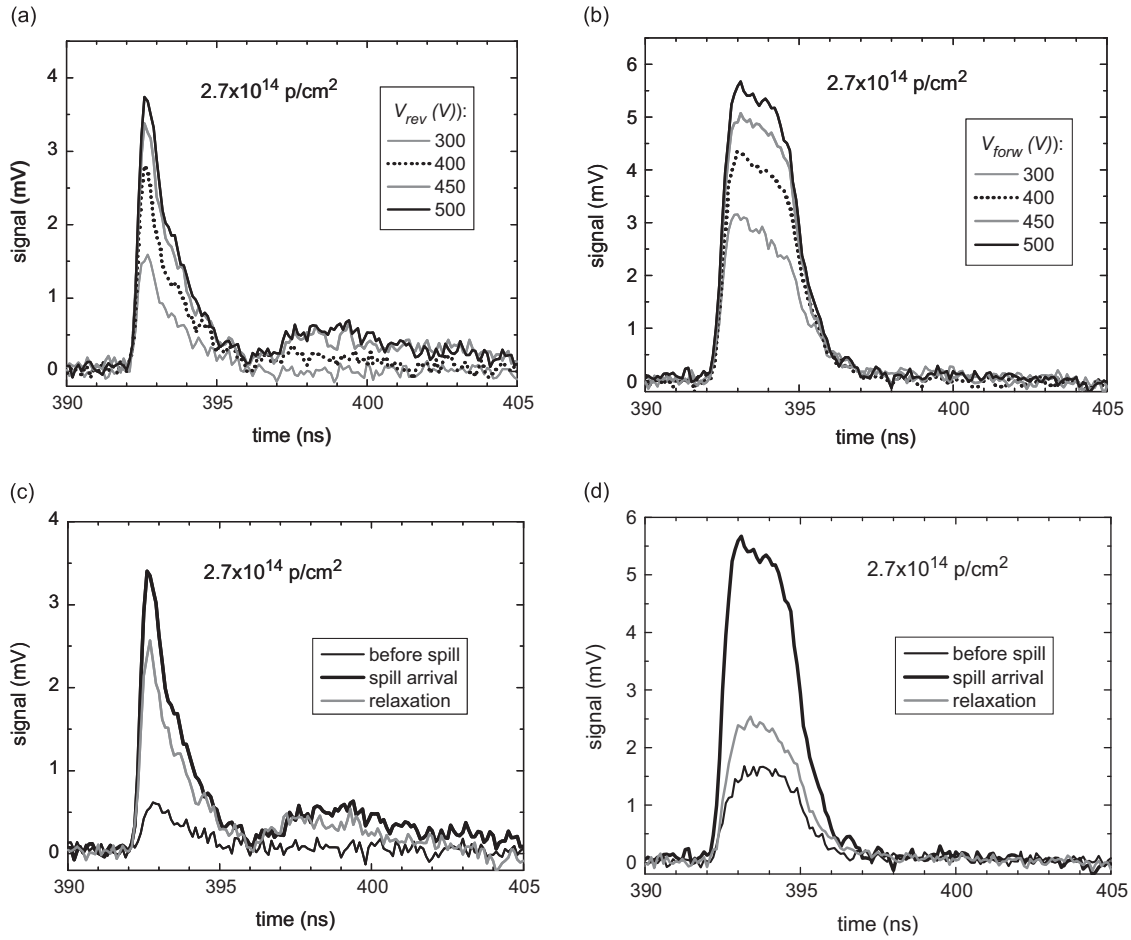

Fig. 5. Current pulse response of silicon detectors irradiated at 1.9 K recorded at spill arrival at different V_{rev} and V_{forw} (a and b, respectively), and comparison of the signals before a spill and at the spill arrival at V_{rev}=450 V (c) and V_{forw}=400 V (d).

fluence dependence

$$\tau_{e,h}^{-1} = \beta_{e,h} F \tag{3}$$

where $\beta_{e,h}$ are the proportionality constants for electrons and holes, respectively, with values at *RT* included in the range $(3.2–5.5)\times 10^{-16}$ cm^2 ns^{-1} [18,19]. The problem arising in the simulation/fitting is in that the values of β at 1.9 K are not known; therefore we used them as tuned parameters derived from the fits. Taking into account the data on the current pulse response described in Section 3, *i.e.* the rapid degradation of the detector signals with fluence, it was assumed that the values of τ must be lower than at *RT* and, *vice versa*, the parameters β must be greater. The dependences of the carrier mobilities on *T* were approximated as in [20].

The experimental $Q_c(F)$ dependences for a detector operated at $V=\pm 300$ V and the corresponding fits at 1.9 K are shown in Fig. 8. The fits are performed with the constraint $\tau_h < \tau_e$ in accordance with the TCT data. In order to fit the experimental data with Eq. (2) we had to use higher values for the parameters $\beta_{e,h}$, and the fits gave the following values

$$\beta_e = 6\times 10^{-15}\ \text{cm}^2\ \text{ns}^{-1}, \beta_h = 9\times 10^{-15}\ \text{cm}^2\text{ns}^{-1}\ \text{at}\ V_{rev}$$

$$\beta_e = 2.2\times 10^{-15}\ \text{cm}^2\ \text{ns}^{-1}, \beta_h = 7\times 10^{-15}\ \text{cm}^2\ \text{ns}^{-1}\ \text{at}\ V_{forw}$$

which are at least seven times higher than at *RT*. The deviation of the experimental $Q_c(F)$ curves from the fits is within the experimental accuracy of $\pm$15%. For comparison, the $Q_c(F)$ dependence simulated for radiation degradation of the collected charge at *RT* is also shown. Another evidence for the introduction during irradiation at 1.9 K of acceptor-like defects in addition to donor-like ones is the fit dependence on both trapping constants.

As mentioned above, the fits to the experimental data were performed using the assumption of a uniform electric field distribution. However, according to the results presented in Section 3.2, the electric field is likely to be nonuniform. The assumption concerning a prevailing formation of interstitial-related defects (hole traps) based on the referred data [5,6] does not seem undisputable, because the pulse response shapes evidently show DP shape and SCSI, which indicates accumulation of the negative charge near the n^+ contact. Nonuniformity in the electric field profile can, in turn, give impact on the values of the trapping time constants derived from the fits.

5. Conclusions

Silicon detectors were proposed for the upgrade of the Beam Loss Monitoring system at the LHC at CERN: they would be installed close to the superconducting coils of the triplet magnets inside superfluid helium. The data on the current pulse response and charge collection in silicon detectors obtained in the first test of *in situ* irradiation by 23 GeV protons at 1.9 K showed that detectors remain operational in these specific conditions up to the fluence of 1×10^{16} p/cm^2.

The fitting of the $Q_c(F)$ dependences was performed using the Hecht equation and the assumption of a uniform electric field distribution at 1.9 K. The results of the study were analyzed, taking into account the specifics of radiation-induced defect formation at low temperature. The main factor responsible for the degradation of the collected charge is related to carrier trapping: the trapping time

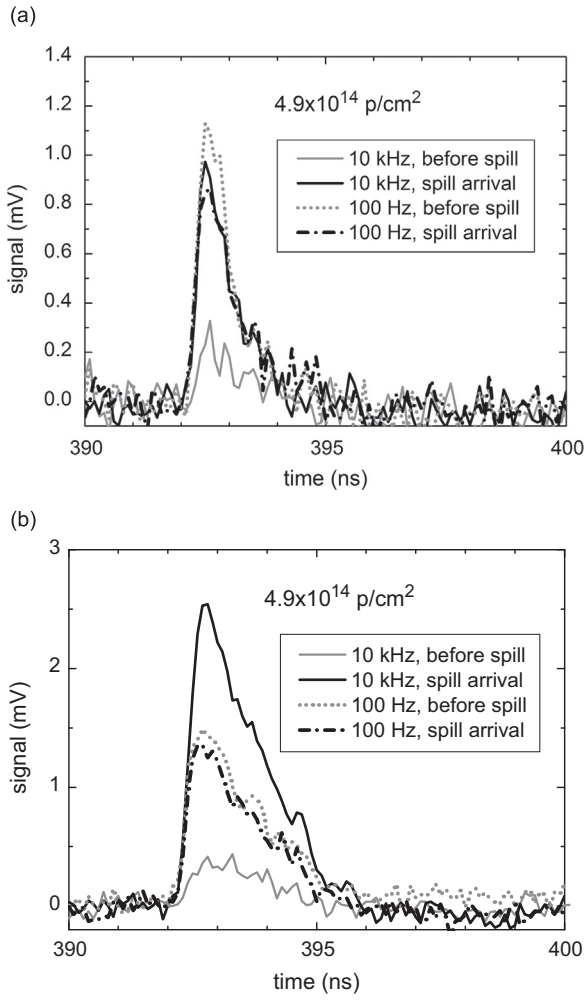

Fig. 6. Influence of spill charge and laser frequency on the current pulse response of silicon detector irradiated at 1.9 K. (a) V_{rev}=450 V; (b) V_{forw}=400 V.

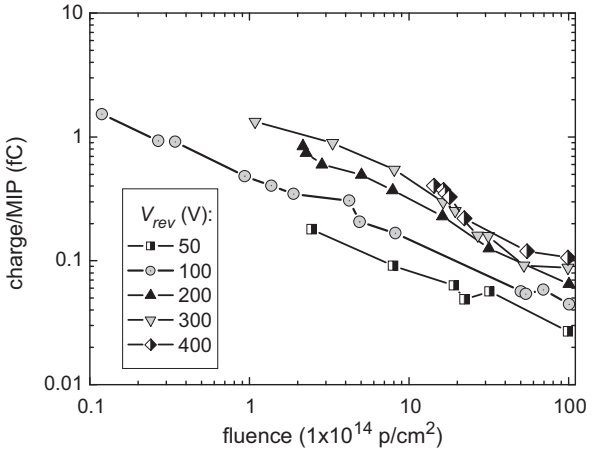

Fig. 7. Experimental $Q_c(F)$ dependences for the detector from 10 kΩ cm silicon operated at reverse bias voltage and irradiated at 1.9 K.

constants are lower than at *RT*, and the trapping of holes on the donor-type radiation-induced defects is dominating. This behavior is expected in silicon detectors irradiated at such low temperatures. However, the experimental data on the current pulse response give grounds to say that, along with formation of donors, acceptor-type

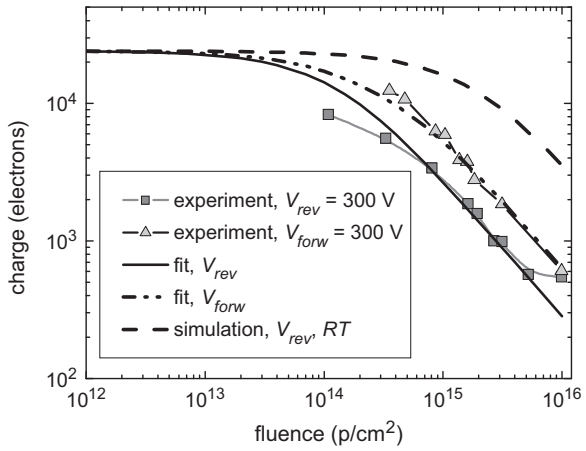

Fig. 8. Experimental $Q_c(F)$ dependences for the detector irradiated at 1.9 K and the corresponding fits.

defects are likely to be introduced inside the silicon bulk. This view is due to space charge sign inversion which was observed at a fluence similar to that for *RT* irradiation.

As far as this assumption is concerned, there is a qualitative agreement between the experimental data and calculated results. On the other hand, it is clear now that the models developed for simulation of the processes in irradiated silicon detectors and their characteristics require an extension for trapping at low *T* with a contribution of shallow levels, as well as the influence of the carriers introduced by the proton beam of the collider, to be taken into account. This, however, is beyond the scope of this study. Obviously, more *in situ* irradiation tests are needed and planned now to extend statistics of the results and gain a deeper insight into the physics of low temperature detector operation in harsh radiation environment.

Acknowledgments

This work was performed within the framework of Agreement on Scientific Collaboration between CERN-BE-BI-BL group and Ioffe Institute and in the scope of the CERN-RD39 collaboration program, and supported in part by the Fundamental Program of Russian Academy of Sciences, No 11P, project 3.2, on collaboration with CERN. The authors express deep gratitude to I. Menina for linguistic assistance in revision of the text.

References

[1] Y. Unno, et al., Nucl. Instrum. Methods A 650 (2011) 129.
[2] A. Mereghetti, M. Sapinski, Fluka simulations for assessing thresholds of BLMs around the LHC triplet magnets, in: Proceedings of the Cryogenic Beam Loss Monitors Workshop, CERN, Geneva, Switzerland, October 2011, ⟨http://indico.cern.ch/event/CryoBLM2011⟩.
[3] M.R. Bartosik, et al., Cryogenic beam loss monitors for the superconducting magnets of the LHC, CERN-BE-2014-009 BI, ⟨http://cds.cern.ch/record/1972049⟩.
[4] C. Kurfürst, et al., Investigation of the use of silicon, diamond and liquid helium detectors for beam loss measurements at 2 K, in: Proceedings of the IPAC2012, New Orleans, USA, May, 2012, pp. 1080.
[5] G.D. Watkins, Defects and diffusion in silicon processing, in: T.D. De la Rubia, S. Coffa, P.A. Stolk, C.S. Rafferty (Eds.), Proceedings of the MRS Sypm. Proc. Vol. 469, Pittsburgh, 1997, pp. 139.
[6] G.D. Watkins, Phys. Solid State 41 (1999) 746.
[7] M.R. Bartosik, et al., Characterization of Si detectors for the use at 2 K, in: Proceedings of the IPAC2013, Shanghai, China, May 12–17, 2013, pp. 643.
[8] C. Kurfürst, Cryogenic Beam Loss Monitoring for the LHC Dissertation, TU Wien, Geneva, 2013, November.
[9] C. Kurfürst, et al., Nucl. Instrum. Methods Phys. Res. A 782 (2015) 149.
[10] F. Ravotti, M. Glaser, M. Moll, IEEE Trans. Nucl. Sci. NS53 (2006) 2016.
[11] V. Eremin, N. Strokan, E. Verbitskaya, Z. Li, Nucl. Instrum. Methods A 372 (1996) 388.

[12] V. Eremin, J. Härkönen, Z. Li, E. Verbitskaya, Nucl. Instrum. Methods A 583 (2007) 91.
[13] E. Verbitskaya, V. Eremin, Z. Li, J. Härkönen, M. Bruzzi, Nucl. Instrum. Methods A 583 (2007) 77.
[14] Z. Li, et al., Nucl. Instrum. Methods Phys. Res. A 598 (2009) 416.
[15] V. Eremin, E. Verbitskaya, Z. Li, Nucl. Instrum. Methods A 476 (2002) 556.
[16] M. Lampert, P. Mark, Current Injection in Solids, Academic Press, NY, London, 1970.
[17] R.N. Williams, E.M. Lawson, Nucl. Instrum. Methods 120 (1974) 261.
[18] G. Kramberger, V. Cindro, I. Mandić, M. Mikuž, Nucl. Instrum. Methods A 579 (2007) 762.
[19] I. Mandić, A. Gorišek, G. Kramberger, M. Zavrtanik, Nucl. Instrum. Methods A 612 (2010) 474.
[20] V. Eremin, Z. Li, S. Roe, G. Ruggiero, E. Verbitskaya, Nucl. Instrum. Methods A 535 (2004) 622.